Dynamic Material Properties of the Post-Mortem Human Colon

Meghan K. Howes and Warren N. Hardy

Abstract Dynamic equibiaxial tension tests were conducted on cruciate tissue samples obtained from the colon of four human cadavers. Tissue samples were stretched to failure using a custom equibiaxial test device. Load, acceleration, sample thickness, and the displacement of optical markers on the sample surface were recorded throughout the duration of each test. The stress-strain response was quantified for 21 colon tests conducted at an average maximum principal strain rate of 69.2 ± 16.0 s^{-1}. The data indicated regional and directional variations in colon material response. The average Green-Lagrange failure strain was 0.158 ± 0.036 and 0.139 ± 0.039 in the circumferential and longitudinal directions, respectively. The average 2nd Piola Kirchhoff stress at failure was 2.35 ± 1.37 MPa in the circumferential direction and 3.20 ± 1.51 MPa in the longitudinal direction. An increased resistance to stretch was observed in the longitudinal direction with a greater average failure stress and lower average failure strain compared to the circumferential direction. Regional response variations included a lower tensile strength for the descending colon compared to the other regions in both the longitudinal and circumferential directions. Data from this study characterize the biomechanical response of the human post-mortem colon at strain rates expected to be experienced in motor vehicle collisions.

Keywords Biaxial, colon, cadaver, soft tissue, high-rate, tension

I. INTRODUCTION

Clinical data and field accident analysis have indicated an increase in the occurrence of hollow visceral injury in belted occupants in motor vehicle collisions (MVCs) [1-3], despite the risk of serious injury in MVCs being substantially reduced with the proper use of seatbelts [4]. The colon is vulnerable to injury from seatbelt loading and abdominal impact with interior vehicle components due to its location around the periphery of the abdomen. Crash-induced colon injuries include lacerations, perforations, and de-vascularization injuries [5]. The purpose of this study was to characterize the biomechanical response of the colon associated with these failure modes by quantifying the multidirectional stress and strain relationships of tissue samples tested to failure in equibiaxial tension.

Existing material properties data for the human post-mortem large intestine are limited to the uniaxial, quasi-static tensile response [6-7]. Due to the viscoelastic nature of soft tissues, a different response is expected for tissue samples tested at the higher loading rates that would be experienced in MVCs. However, no data exist that characterize the dynamic response of the human colon. Additionally, uniaxial tests are typically conducted without constraint in the transverse direction. This affects the mechanical environment of the sample, particularly for the highly deformable membranous abdominal tissues such as the intestines. The mechanical environment of a planar biaxial test more accurately matches multi-axial loading expected *in vivo*. Further, biaxial tests are necessary to determine the multidirectional stress and strain relationships that cannot be inferred from a uniaxial test due to tissue anisotropy [8]. In this study, dynamic equibiaxial tissue testing was conducted to define the high-rate, multidirectional material response and failure properties of the human post-mortem colon.

*M. K. Howes is a PhD candidate in Biomedical Engineering & Sciences at Virginia Tech-Wake Forest University in Blacksburg, Virginia. (540 231 1890, mkhowes@vt.edu). W. N. Hardy is a Professor of Mechanical Engineering and Director of the Virginia Tech-Wake Forest University Center for Injury Biomechanics at Virginia Tech in Blacksburg, Virginia.

II. METHODS

Surrogate Characteristics

Equibiaxial tension tests were conducted on colon tissue samples obtained from the digestive tract of four fresh, never-frozen post-mortem human surrogates (PMHS). Donors were screened to avoid medical conditions that could potentially affect the material response of the abdominal soft tissues. All surrogates were male and had an average age of 76 years, average stature of 179 cm, and average mass of 93 kg (Table 1).

TABLE 1: PMHS CHARACTERISTICS.

Cadaver	Gender	Age	Stature (cm)	Mass (kg)
SM78	M	77	175	81
SM79	M	72	193	142
SM80	M	72	173	72
SM82	M	81	174	78
Average		76	179	93

Sample Preparation

The colon is divided into four anatomic regions: the ascending, transverse, descending, and sigmoid colon. The colonic wall structure remains consistent throughout the length, consisting of an inner mucosal layer, submucosa, muscularis externa, and outer serosal layer [9]. Thin bands of muscle fibers known as teniae coli extend axially along the length of the colon. The segments of tissue forming the sections between the bands are known as haustra coli.

The excised colon of each surrogate was divided into rectangular tissue sections devoid of visible inhomogeneities. Tissue sections were opened along the mesenteric border aligned with the longitudinal axis of the organ. A custom CNC-machined stamp was applied to the tissue sections using an arbor press. The stamp was designed to produce cruciate-shaped samples with four arm branches converging to form a 10-mm central square region of interest (ROI). Radiused edges between adjacent arm branches reduced stress concentrations at the edges of the ROI. The stamp was aligned with two co-linear arms oriented parallel to the visible longitudinal fiber direction of each tissue section or offset from the fiber direction by 22 degrees (Figure 1). The offset was selected to minimize error in material parameter determination [10] and to prevent failure across the arm branches of the sample [11]. Therefore, the majority of the samples were tested in the offset configuration, and a limited number of samples were tested in the aligned configuration for comparison. All samples were obtained with the layered wall structure intact.

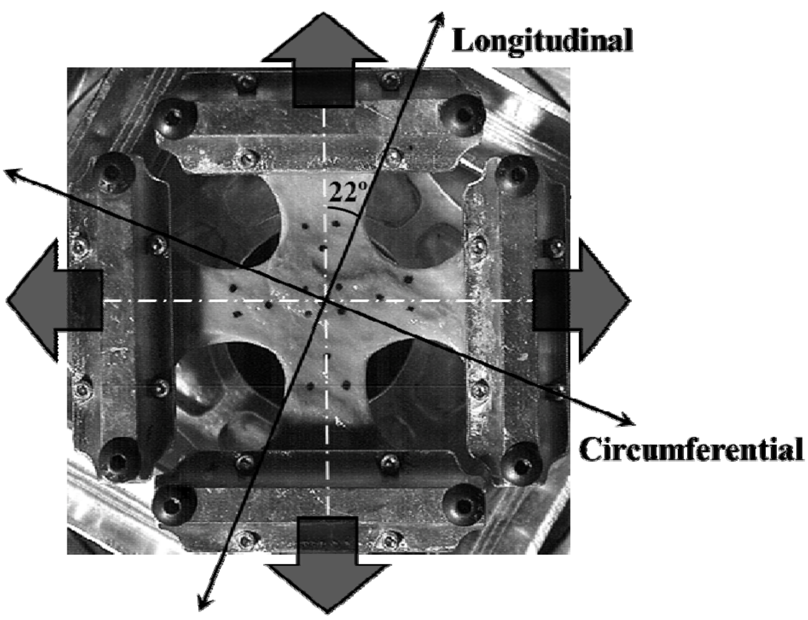

Fig. 1. Colon sample alignment in an offset configuration.

Procurement to testing time was minimized for all tissue samples. Tissues were stored in saline-soaked gauze in airtight containers at 1°C between procurement and testing. Normal saline spray was used to maintain sample hydration during sample positioning and testing. All testing was conducted at ambient temperature.

Test Configuration

Biaxial testing was conducted using a custom test device designed to apply multidirectional strain to cruciate samples at high rates (Figure 2). A detailed description of the device is given by Mason et al. [12]. Sample arms were gripped in four low-mass tissue clamps designed to reduce inertial effects at less than 16 grams for each assembly. The upper and lower edges of each clamp were offset from one another, with knurled surfaces to limited slip at the interface between the tissue sample and the clamp. Threaded rods were used to mount each clamp to a corresponding lightweight carriage equipped with low-friction bearings riding on linear rails. Carriages were rigidly coupled to a central drive disk such that rotation of the disk resulted in simultaneous outward motion of the carriages. Rotation of the disk was generated by a hydraulic actuating mechanism rigidly linked to a lower carriage of the test device and loaded by a falling mass [13].

Miniature load cells (ELFF-T2E-100lb, Measurement Specialties, CA) were used to measure applied load at each tissue clamp. Miniature accelerometers (3038-500g, Measurement Specialties, CA) were mounted to each carriage for inertia compensation of the measured load. Laser displacement sensors (LK-G157, Keyence Corporation, NJ) mounted above and below the sample were used to obtain sample thickness in the ROI throughout the duration of each test. Sample thickness was calculated using a calibrated difference in recorded measurement from the upper and lower sensors. All data were captured using 20 ksps. Overhead high-speed video (Phantom v9.1, Vision Research, NJ) captured using 2500 fps provided optical data in the ROI of the sample at a resolution of 7 px/mm.

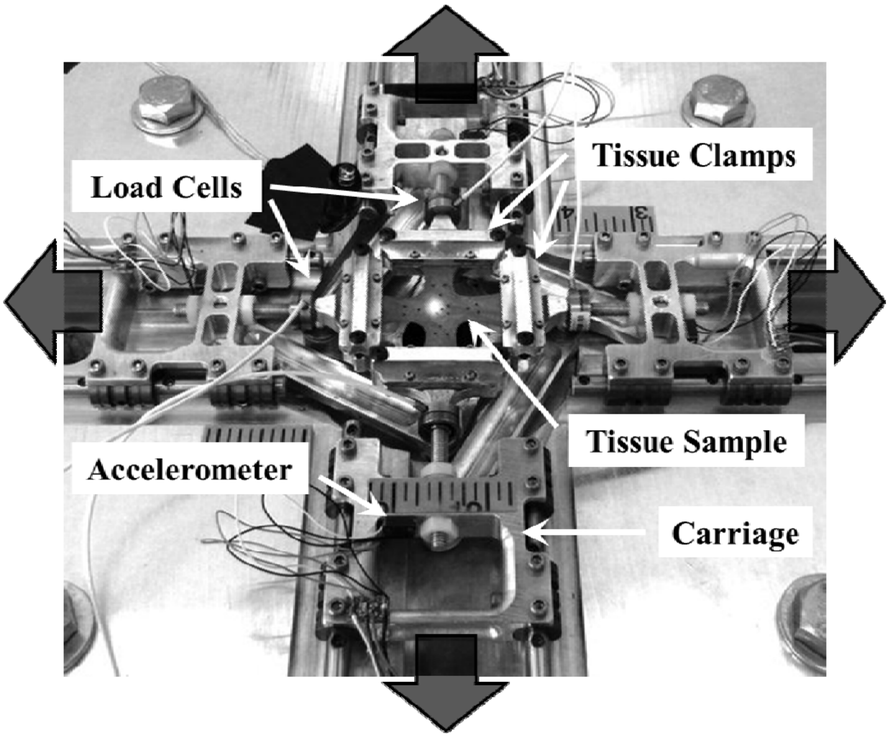

Fig. 2. Biaxial tissue test device.

Colon samples were positioned in the test device with the inner mucosal layer in view of the high-speed video camera. Prior to positioning the sample, the carriage assemblies were adjusted to the inward position, and each clamp was adjusted using the threaded rods to ensure that all clamps were equidistant from the center of the test device. Samples were transferred to a foam block upon which the ROI was supported to ensure minimal deformation occurred during positioning. Sample arms were aligned with the centerline of each lower clamp and positioned maintaining equal arm length to the center of the ROI. Once aligned, the upper clamps were applied and tightened, and the foam support was removed from beneath the sample. To maintain repeatable initial conditions, the clamps were individually adjusted using the threaded rods to reduce any remaining slack in the sample. A pattern of 17 optical markers was applied to the sample surface using indelible ink. Samples were stretched at a target strain rate of 100 s^{-1} until complete transection occurred. This target rate was selected based on the results of Hardy et al. [14], where the instantaneous strain rates in the cadaver aorta exceeded 50 s^{-1} in dynamic impact tests that simulated loading in MVCs.

Data Processing and Analysis

Data included in this study expand upon the Green-Lagrange strain data presented in [13] with the characterization of the directional stress-strain response to failure for tissue samples obtained from all regions of the colon. All data were zeroed at the time corresponding to the initiation of carriage movement determined from high-speed video analysis. Failure was defined as tear initiation identified using the high-speed video. All data were truncated at the time of tear initiation as the purpose of this work was to obtain response and tolerance to failure, and the subsequent tear propagation requires a more complex analysis. If a peak in the load-time history preceded tear initiation, data were then truncated at the time of peak load filtered using SAE J211 CFC 600 Hz [15].

Multidirectional displacement data were obtained by tracking the position of five markers in the ROI using motion analysis software (TEMA, Image Systems, Linköping, Sweden) employing a regional correlation method. Displacement data for each marker were input into LS-DYNA as boundary prescribed motion for five nodes. Each triad of nodes sectioned the ROI into four triangular shell elements. Green-Lagrange strain, maximum principal strain, and maximum shear strain were determined as the average value from each of the four elements solved at 0.05 ms time intervals. Green-Lagrange strain for each element corresponds to the strain tensor (Eqn. 2) calculated from the deformation gradient computed for each triad (Eqn. 1). The stretch ratio (λ) and true strain (ε) were calculated from the Green-Lagrange strain (Eqn. 3). Maximum principal strain corresponds to the eigenvalues (λ±) of the Green-Lagrange strain tensor (Eqn. 4). Average maximum principal strain rate was calculated as the average of the time derivative of the maximum principal strain over the test duration. All strain data were transformed to align with the material axes of the tissue.

$$\mathbf{F} = \left(\begin{bmatrix} \mathrm{X}_1 & \mathrm{X}_2 \\ \mathrm{Y}_1 & \mathrm{Y}_2 \end{bmatrix}_{t=1}\right)\left(\begin{bmatrix} \mathrm{x}_1 & \mathrm{x}_2 \\ \mathrm{y}_1 & \mathrm{y}_2 \end{bmatrix}_{t=0}\right)^{-1} \quad \text{(Eqn. 1)}$$

$$\mathbf{E} = \begin{bmatrix} \mathrm{E}_{11} & \mathrm{E}_{12} \\ \mathrm{E}_{21} & \mathrm{E}_{22} \end{bmatrix} = \frac{1}{2}(\mathrm{F}^{\mathrm{T}}\mathrm{F} - \mathrm{I}) \quad \text{(Eqn. 2)}$$

$$\varepsilon = \ln\lambda = \ln\sqrt{2\mathrm{E}+1} \quad \text{(Eqn. 3)}$$

$$\lambda_{\pm} = \frac{1}{2}\left[(\mathrm{E}_{11}+\mathrm{E}_{22}) \pm \sqrt{4\mathrm{E}_{12}\mathrm{E}_{21} + (\mathrm{E}_{11}-\mathrm{E}_{22})^2}\right] \quad \text{(Eqn. 4)}$$

Calculation of the load applied to the ROI in each direction was dependent on inertia compensation and scaling of the measured load. The effective mass used for inertia compensation was optimized for each of the four measured loads for each tissue test. Compensated load for each clamp was adjusted to the ROI by applying an assumption of a proportional transmission of load through each arm to the central region. A scaling ratio of the initial length of the ROI, obtained as the distance between the outer marker pairs, to the initial sample arm width in the same direction was applied to scale the normal load at each time step. The resulting values were taken as the load applied to the ROI. Two compensated loads in each direction were averaged to obtain the load-time history in the x- and y-directions.

True stress (S) was calculated by first determining changing cross-sectional area (A_n) for each sample. Laser thickness data filtered using SAE J211 CFC 180 Hz [15] was multiplied by the average ROI length, determined in each direction. In the event that the laser thickness data were confounded by sample surface inhomogeneities, an assumption of incompressibility (Poisson's ratio equal to 0.5) was used to calculate changing sample thickness by assuming volume conservation. The validity of this assumption was investigated by Shah et al. [11] using samples from the cadaver aorta, although greater variability would be expected for colon samples due to the presence of inhomogeneities on the upper and lower surfaces of the samples. The unfiltered load (P) applied to the region of interest in each direction was divided by the appropriate cross-section to obtain true stress (Eqn. 5). 2nd Piola Kirchhoff stress (K) was determined using the unfiltered applied load (P), the initial cross-section (A_0), and the inverse of the stretch ratio (λ) in the appropriate directions (Eqn. 6). Stress data were filtered using SAE J211 CFC 600 Hz [15]. All stress data were transformed to align with the material axes of the tissue.

$$S = \frac{P}{A_{n_\perp}} \quad \text{(Eqn. 5)}$$

$$K = \frac{P}{A_{0_\perp}} * \frac{1}{\lambda_\parallel} \quad \text{(Eqn. 6)}$$

Within each region, the circumferential and longitudinal failure strains were compared using two-sample Student's t-tests assuming unequal variances (α=0.05). Single factor ANOVA (α=0.05) was used to compare failure strain between regions for each direction. Identical statistical comparisons were made for failure stress.

III. RESULTS

A total of 38 equibiaxial tension tests were conducted on colon samples obtained from four PMHS. The final dataset consisted of 21 tests meeting inclusion criteria of sample uniformity in each direction and failure tear initiation at the edge of the ROI. The average maximum principal strain rate for all tests was 69.2 ± 16.0 s^{-1}. For the majority of the tests, the failure strain was greater in the circumferential direction compared to the longitudinal direction. The average Green-Lagrange failure strain in the circumferential direction was 0.158 ± 0.036, and the average failure strain in the longitudinal direction was 0.139 ± 0.039. Average 2nd Piola Kirchhoff stress at failure was 2.35 ± 1.37 MPa and 3.20 ± 1.51 MPa in the circumferential and longitudinal directions, respectively. The maximum shear strain at failure was approximately 10-percent on average for all tests.

The final dataset included 3 samples from the ascending colon, 4 from the transverse colon, 7 from the descending colon, and 7 from the sigmoid colon. Figure 3 and Figure 4 show the directional Lagrangian stress-strain response for each region of the colon. The aligned (N=7) and offset (N=14) sample groups are differentiated in Figure 3 and Figure 4. In general, the samples aligned with the long axis of the tissue showed a decreased stiffness in the circumferential direction compared to samples that were offset by 22 degrees. This result was not observed in the longitudinal direction. Due to the low sample size, the aligned and offset samples were considered together for the remainder of the analysis.

In all regions, the average failure strain was greater in the circumferential direction than in the longitudinal direction. However, there were no statistically significant directional differences in failure strain within each region (Table 2). Further, no statistically significant differences in failure strain were found between regions in either the circumferential (p=0.34) or the longitudinal direction (p=0.59) using single factor ANOVA (Table 4). Average failure stress was greater in the longitudinal direction for all regions of the colon. No statistically significant differences were found in 2nd Piola Kirchhoff failure stress by direction within each region; however, the greatest differences in directional failure stress were observed within the transverse and sigmoid regions (Table 3). There was a statistically significant difference in longitudinal failure stress between regions of the colon (p=0.01) as determined by single factor ANOVA (Table 4). Post hoc analyses using the Tukey-Kramer multiple comparisons test indicated that the longitudinal failure stress for the descending colon was significantly lower than for the sigmoid colon (p<0.05). No other comparisons were significant. Results for true stress and true strain are provided in the Appendix (Tables A1-A2).

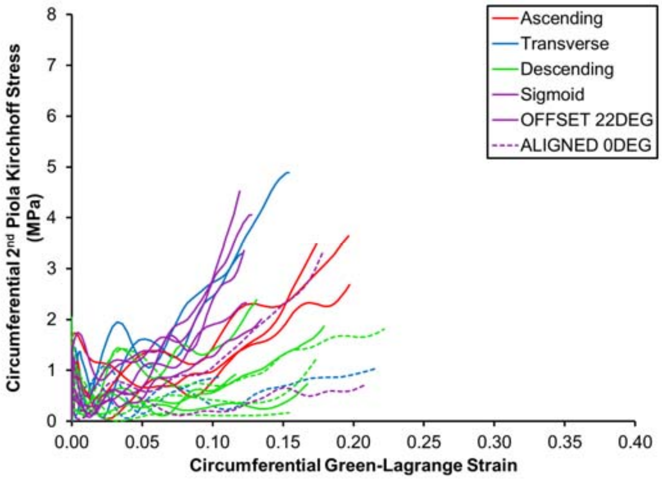

Fig. 3. Circumferential stress-strain response by region.

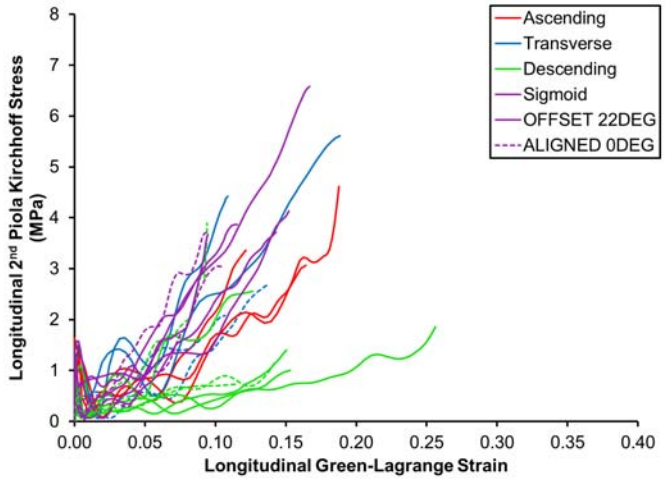

Fig. 4. Longitudinal stress-strain response by region.

TABLE 2: GREEN-LAGRANGE FAILURE STRAIN BY REGION.

Region	N	Circumferential Failure Strain		Longitudinal Failure Strain		p-value
		AVG	STDEV	AVG	STDEV	
Ascending	3	0.189	0.013	0.158	0.034	0.25
Transverse	4	0.149	0.049	0.135	0.038	0.67
Descending	7	0.163	0.034	0.148	0.052	0.54
Sigmoid	7	0.145	0.035	0.124	0.029	0.26
Total	21	0.158	0.036	0.139	0.039	0.11

TABLE 3: 2ND PIOLA KIRCHHOFF FAILURE STRESS BY REGION (MPa).

Region	N	Circumferential Failure Stress		Longitudinal Failure Stress		p-value
		AVG	STDEV	AVG	STDEV	
Ascending	3	3.27	0.52	3.68	0.82	0.51
Transverse	4	2.53	1.92	3.70	1.61	0.39
Descending	7	1.31	0.77	1.80	1.10	0.35
Sigmoid	7	2.90	1.31	4.10	1.14	0.09
Total	21	2.35	1.37	3.20	1.51	0.06

TABLE 4: ANOVA COMPARISONS BETWEEN REGIONS.

Parameter	Circumferential p-value	Longitudinal p-value
Green-Lagrange Strain	0.342	0.591
True Strain	0.332	0.581
2nd Piola Kirchhoff Stress	0.073	**0.012**
True Stress	**0.047**	**0.027**

IV. DISCUSSION

Multidirectional stress-strain responses were quantified for 21 equibiaxial tissue tests conducted using post-mortem colon samples. An increased resistance to stretch was observed in the longitudinal direction with a greater average failure stress and lower average failure strain compared to the circumferential direction. A stiffer response in the longitudinal direction may be attributed to a lower resistance to stretch in the circumferential direction, related to the physiologic need for expansion of the colon during digestion. Further, stretch in the longitudinal direction may be inhibited by the muscular teniae coli extending axially throughout the length of the large intestine.

Similar trends were found in uniaxial tension tests conducted at constant quasi-static strain rates [6-7]. The results of the current study were consistent with the findings of Egorov et al. [7] in which an increase in stress occurred at a lower percent strain for longitudinal teniae samples. This indicated a greater resistance to stretch for the teniae samples compared to longitudinal haustra samples and intact transverse samples. Yamada [6], citing [16], reported for all regions of the colon a greater ultimate percent elongation in the circumferential direction and a higher ultimate strength in the longitudinal direction.

Regional variations in mechanical response were also observed in this study. Failure strain, on average, was greatest for the ascending colon, followed by the descending colon, transverse colon, and sigmoid colon for both the circumferential and longitudinal directions. These differences, however, were minimal and not significant. Average failure stress for the descending colon was considerably lower than for the other regions. This result was only significant compared to the sigmoid colon in the longitudinal direction. Yamada [6], citing [16], also reported the lowest ultimate stress for the descending colon compared to the other regions of the large intestine. Despite similarities in wall structure between all regions of the colon, physiologic differences may contribute to the observed regional variations in mechanical response.

Assumptions and Limitations

Load was applied to the tissue samples a distance away from the ROI where stress and strain were calculated. In order to transfer the measured load to the ROI, assumptions of a uniform stress distribution within the sample and a proportional transmission of load from the tissue clamps to the central region were applied. Small samples without visible defects were tested in an attempt to ensure that the samples were devoid of any large-scale inhomogeneities. Future work will include an assessment of the equality of the load distribution in each direction for the tissue samples. Additionally, load applied at the edge of each of the sample arms must propagate to the central region over time. It was assumed for these tests that the small sample size minimized the effect of load application a distance away from the ROI, and therefore an instantaneous transmission of load to the ROI occurred. However, the initial stress offset in the stress-strain response curves for the colon can be partially attributed to the load application and measurement at the edges of the arm branches of the sample before stretch occurred in the ROI.

The ability to obtain repeatable and uniform sample geometry for component-level tissue tests is confounded by the compliant nature of the tissue; however, shear strain was used to characterize this limitation. Uneven sample geometry, slip between sample layers, and rotation or vibration of the sample arms increases the shear strain. Shear strain was minimized in this study by maintaining short and equal sample arm length and ensuring even geometry for all four arms. The target maximum shear strain of ten-percent prior to tissue failure was considered reasonable for these tests, indicating that multi-axial stretch was achieved with minimal shear in the ROI.

The samples aligned with the material axes of the tissue and those offset from the long axis by 22 degrees were considered together for this analysis due to the low number of samples obtained from each region of the colon. A stiffer response was expected for the offset samples; however, this trend was only observed in the circumferential direction. It is likely that additional regional differences in directional failure properties would be apparent if the sample size within each region was increased and only the offset samples were considered for analysis.

The results of component-level tissue testing are only applicable *in vitro* and do not directly describe the *in vivo* response of the tissue. Although efforts were made to maintain repeatable initial test conditions for all samples, these conditions may not match the physiologic stress or strain state occurring *in vivo*. Further, the response of the tissue samples measured in a small central ROI may not be representative of the *in vivo* response of the whole organ [8]. Despite these limitations, acquiring equibiaxial response data contributes to material property validation at the component-level with an approach more representative of the complex, multi-axial behavior expected *in vivo.*

V. CONCLUSIONS

Limited material properties data are available in the literature for the complex anatomical structures of the digestive system. These data were obtained at quasi-static loading rates that are not representative of the dynamic loading rates experienced in MVCs. In this study, material properties and failure thresholds of colon samples were obtained in equibiaxial stretch at loading rates expected to be experienced in MVCs. These tests were designed to account for the high strain rate, large deformation behavior of the material and to include the anisotropic tissue response. The average Green-Lagrange failure strain was 0.158 ± 0.036 and 0.139 ± 0.039 in the circumferential and longitudinal directions, respectively. The average 2nd Piola Kirchhoff stress at failure was 2.35 ± 1.37 MPa in the circumferential direction and 3.20 ± 1.51 MPa in the longitudinal direction. The overall stress-strain response indicated an increased resistance to stretch in the longitudinal direction with a greater failure stress and lower failure strain compared to the circumferential direction. Stress and strain response data quantified in this study provide new biomechanical data at rates useful for finite element impact simulations designed to evaluate crash-induced abdominal organ injury.

VI. ACKNOWLEDGMENT

A portion of this work was funded by the Global Human Body Models Consortium, LLC.

VII. REFERENCES

[1] Anderson PA, Rivara FP, Maier RV, Drake C, The epidemiology of seatbelt-associated injuries, *J Trauma,* 31: 60-67, 1991.

[2] Rutledge R, Thomason M, et al., The spectrum of abdominal injuries associated with the use of seat belts, *J Trauma,* 31: 820-826, 1991.

[3] Lamielle S, Cuny S, et al., Abdominal injury patterns in real frontal crashes: influence of crash conditions, occupant seat and restraint systems, *Annu Proc Assoc Adv Automot Med,* 50: 109-124, 2006.

[4] Klinich KD, Flannagan CAC, Nicholson K, Schneider LW, Rupp JD, Factors associated with abdominal injury in frontal, farside, and nearside crashes, *Stapp Car Crash J,* 54: 73-91, 2010.

[5] Carrillo EH, Somber LB, et al., Blunt traumatic injuries to the colon and rectum, *J Am Coll Surg,* 183: 548-552, 1996.

[6] Yamada H, Strength of Biological Materials, pp. 191-194, *The Williams & Wilkins Company,* Baltimore, 1970.

[7] Egorov VI, Schastlivtsev IV, Prut EV, Baranov AO, Turusov RA, Mechanical properties of the human gastrointestinal tract, *J Biomech,* 35: 1417-1425, 2002.

[8] Sacks MS, Biaxial mechanical evaluation of planar biological materials, *J Elasticity,* 61: 199-246, 2000.

[9] Ross MH and Pawlina W, Histology: Text and Atlas, 6th Edition, *Lippincott Williams & Wilkins,* Philadelphia, 2011.

[10] Lanir Y, Lichtenstein O, Imanuel O, Optimal design of biaxial tests for structural material characterization of flat tissues, *J Biomech Eng,* 118: 41-46, 1996.

[11] Shah CS, Hardy WN, et al., Dynamic biaxial tissue properties of the human cadaver aorta, *Stapp Car Crash J,* 50: 217-246, 2006.

[12] Mason MJ, Shah CS, et al., A new device for high-speed biaxial tissue testing: application to traumatic rupture of the aorta, *SAE World Congress,* Detroit, MI, SAE Paper No. 2005-01-0741, 2005.

[13] Howes MK and Hardy WN, Material properties of the post-mortem colon in high-rate equibiaxial elongation, *Biomed Sci Instrum,* 48: 171-178, 2012.

[14] Hardy WN, Shah CS, et al., Mechanisms of traumatic rupture of the aorta and associated peri-isthmic motion and deformation, *Stapp Car Crash J,* 52: 233-265, 2008.

[15] Society of Automotive Engineers, J211/1 Instrumentation for Impact Test - Part 1 - Electronic Instrumentation, *Society of Automotive Engineers,* Warrendale, PA, 2007.

[16] Iwasaki T, Study on the strength of the human intestinal walls, *J Kyoto Pref Med Univ,* 52: 673-702, 1953.

VIII. APPENDIX

TABLE A1: TRUE FAILURE STRAIN BY REGION.

Region	N	Circumferential Failure Strain		Longitudinal Failure Strain		p-value
		AVG	STDEV	AVG	STDEV	
Ascending	3	0.160	0.010	0.137	0.026	0.25
Transverse	4	0.130	0.037	0.119	0.029	0.67
Descending	7	0.141	0.026	0.129	0.038	0.50
Sigmoid	7	0.127	0.026	0.111	0.023	0.25
Total	21	0.137	0.027	0.122	0.030	0.10

TABLE A2: TRUE FAILURE STRESS BY REGION (MPa).

Region	N	Circumferential Failure Stress		Longitudinal Failure Stress		p-value
		AVG	STDEV	AVG	STDEV	
Ascending	3	4.14	0.84	4.49	1.33	0.73
Transverse	4	2.87	2.20	4.14	2.11	0.44
Descending	7	1.47	0.90	1.95	1.17	0.41
Sigmoid	7	3.39	1.55	4.74	1.87	0.17
Total	21	2.76	1.66	3.66	1.97	0.12